Confocal microwave imaging for breast tumor detection: application to a hemispherical breast model

Elise C. Fear and Michal Okoniewski

Electrical and Computer Engineering, University of Calgary, Calgary AB Canada T2N 14N
email: fear@enel.ucalgary.ca

Abstract — **Confocal microwave imaging (CMI) has been proposed for breast imaging, and detects tumors by selectively focussing backscatter from the breast. Previous studies have employed simple cylindrical or planar breast models, or 2D breast models created from breast MRI scans. In this paper, we use a hemispherical breast model to examine tumor detection and localization in 3D. This model has more realistic features than the simple cylinder. Results indicate that extension of cylindrical CMI to 3D scans of more complex models appears feasible. Future work includes developing methods to accomplish a full breast scan with cylindrical CMI.**

I. Introduction

Breast cancer is a concern for many women. Early detection is essential for comfortable and effective treatment, and is improved by participation in screening programs. Breast screening involves mammography, x-ray imaging of a compressed breast. Many lesions in the breast are detected by mammography, however a significant percentage of lesions are likely missed [1]. Additional concerns include the need for further investigation of suspicious areas that are not conclusively diagnosed by mammography [1]. This has focused interest on alternative methods of breast tumor detection or diagnosis.

Recently, interest in microwave imaging for breast tumor detection has grown. The basis of tumor detection with microwaves is the significant contrast in electrical properties of normal and malignant breast tissues. Passive, active and hybrid approaches to breast imaging have been proposed. Of particular interest to this paper are active approaches. Established practice in active microwave imaging [2] involves illuminating the breast with microwaves, and detecting the energy transmitted through the breast. A model of the breast with estimated electrical properties is used to compute the transmitted energy. The estimated properties are adjusted until the measurements and computations converge. An alternative approach is confocal microwave imaging (CMI). The breast is illuminated with an ultra-wideband pulse of microwaves, and reflections are detected at the illuminating antenna. This is repeated for a number of physical antenna locations, forming an array. Images are formed by synthetically focussing the array, which involves computing the time delay from each antenna to the focal point, then time shifting and summing signals. CMI has the advantage of a simple approach to image reconstruction, however only locates strong scatterers in the breast, rather than providing a map of electrical properties.

Two configurations for CMI are being investigated, planar and cylindrical. With planar CMI, the woman lies on her back and antennas are placed on the flattened breast. With cylindrical CMI, the woman lies on her stomach; the breast extends through a hole in the examination table, and is encircled by an antenna array. To date, much of the reported CMI work has involved computational studies of simple cylindrical or planar breast models. With these simple models, the possibility of detecting and localizing tumors in 3D has been demonstrated [3]. A 2D model created with a breast MRI scan has been used by Li and Hagness to demonstrate 2D detection and localization with a more realistic model [4]. In this paper, a hemispherical model is examined as an intermediate step between simple and realistic 3D models. While this model involves simplifying assumptions, it allows for insight into the performance of cylindrical CMI image reconstruction with a more complex 3D model.

This paper describes the hemispherical model and methods used to reconstruct images with simulated data. Images are presented for a 2D slice through hemispherical models with and without a tumor. Results of a 3D scan are provided, and the implications of these studies are discussed.

II. Methods

A. Models and Simulations

Previous investigations of cylindrical CMI employed a simple, cylindrical breast model. To explore the extension of our algorithms to a more complex situation, the breast model presented in Fig. 1 was developed. Electrical properties are summarized in Table 1. While this model is

0-7803-7239-5/02/$10.00 © 2002 IEEE

not as detailed as, for example, a model created from MRI breast scans, it contains a more realistic shape, nipple, chest wall, and more structured glandular tissue when compared to a cylindrical model. The model also has larger diameter (14 cm compared to 6.8 cm). The more realistic shape allows testing the extension of skin subtraction to a curved surface. The nipple and chest wall are significantly scattering, and are sources of clutter. The glandular tissue has greater contrast with the background tissue than the previously investigated 10%, and contains more structure than previously used cubes.

The breast model is illuminated by a single resistively loaded dipole antenna with a Wu-King profile designed at 4 GHz [5]. The antenna is excited with a differentiated Gaussian signal with maximum frequency content near 4 GHz and approximately 6 GHz bandwidth (full-width half-maximum). Simulations are performed with the finite difference time domain method [6]. To create images of a 2D slice through the model, simulations are performed with the antenna centered on the tumor in the z direction (Fig. 1a). At this height, the antenna is moved to 20 equally spaced locations around the breast. For the 3D scan, an array of 90 antennas is used. The array consists of 9 rows with 10 antennas per row, and rows are separated by 0.5 cm. In all cases, the antennas are placed approximately 1 cm from the skin.

B. Signal Processing

The signal processing algorithm has steps similar to those previously reported [3]. The steps include:

- *calibration,* or subtraction of signals recorded without a breast model present;
- *skin subtraction* to remove the dominant reflection from the layer of skin;
- *integration* to transform the center of the signal from a zero to a maximum;
- *radial spreading compensation* to account for the 1/r decrease in amplitude of the wave with distance from its source; and
- *focussing* to form the image.

Skin subtraction involves aligning signals with respect to the skin reflection, then subtracting the average of the set from each signal. Each set consists of the signals recorded at one antenna height. For the 3D reconstruction, an additional local subtraction step is applied. In this case, the four antennas closest to a selected antenna are identified. The average of the signals at the 5 antennas is taken, and subtracted from the signal at the selected antenna. This is repeated for each antenna location.

Focussing involves computing the time delay from each antenna to a selected focal point, identifying the corresponding components of each signal, then time-shifting and summing the signals. During focussing, additional weighting is applied to the data. Signals from antennas closer to the focal point are given greater weight than signals from antennas that are more distant.

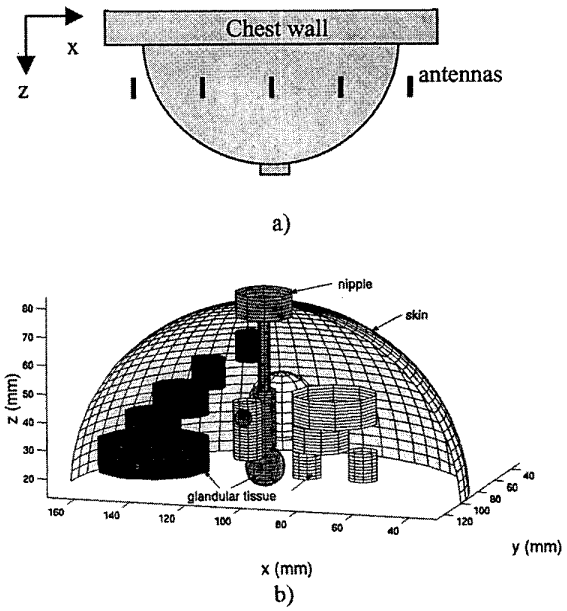

Fig. 1. The hemispherical breast model with diameter of 14 cm. The breast model and antenna are immersed in a low loss liquid. a) The orientations of the chest wall and antenna locations are indicated. b) The interior of the model contains objects representing glandular tissue (blue, green, white, pink and yellow spheres and cylinders). The 6 mm diameter tumor is the small red sphere. The remainder of the space is filled with fatty breast tissue.

TABLE 1
ELECTRICAL PROPERTIES OF TISSUES FOR BREAST MODEL

Tissue	Electrical properties	
	ε_r	σ (S/m)
Immersion liquid	9	0
Chest wall	50	7
Skin	36	4
Fatty breast tissue	9	0.4
Nipple	45	5
Glandular tissue	11-15	0.4-0.5
Tumor	50	4

C. Measures

To examine the influence of each step in the signal processing sequence, the reflections recorded at each antenna are examined. The peak-to-peak tumor response compares the peak-to-peak reflection from the tumor to the peak-to-peak total signal. The peak-to-peak tumor response is obtained by subtracting reflections from a tumor-free breast model and reflections from a breast model with a tumor.

To evaluate tumor detection in images, several approaches are taken. First, 2D images are formed for models with and without tumors to confirm that tumors are only detected when present. Signal-to-clutter (S/C) ratios are computed for the 2D images. To compute the within-breast S/C ratio, the maximum tumor response is compared to the maximum clutter response in the same image. The between-breast S/C ratio is the ratio between the maximum tumor response and the corresponding pixel in the image of the tumor-free breast. The location and size of the tumor response are compared to the physical tumor location and dimensions.

III. Results

To provide assessment of each signal processing step, the peak-to-peak tumor response and total signal for a single antenna are summarized in Table 1. Results for a simple cylindrical model are also included for comparison. For the hemispherical model, the antenna-tumor distance ranges from 4.5 cm to 10.2 cm. For the antenna at 10.2 cm, the initial peak-to-peak ratio is -135 dB, which improves to -31 dB after compensation.

Images are shown in Figs. 2 and 3 for a plane slicing through breast at the tumor location. The between-breast S/C ratio is 4.9 dB. The within-breast S/C ratio is 1.6 dB. The clutter responses in the image correspond to the location of the glandular tissue.

Images are reconstructed for the 3D volume using the 9x10 array. Without the additional local subtraction step, clutter is the dominant component in the images. The tumor is evident, however its response is less than that of the clutter (specifically, the within-breast S/C ratio is -0.84 dB). With the additional local subtraction, the tumor response is the dominant response in the image. Figs. 4 and 5 show images of 2 orthogonal cuts through the maximum tumor response. Clutter is evident, and the within-breast S/C ratio is 0.81 dB. The tumor response at occurs at x=0.122 m, y=0.1 m, z=0.046 m, while the physical tumor location is x=0.125 m, y=0.1 m, z=0.045 m. The tumor response with magnitude greater than the maximum clutter has volume of 16 mm^3.

TABLE 2
TUMOR RESPONSE COMPARED TO TOTAL SIGNAL AFTER EACH SIGNAL PROCESSING STEP. RESULTS FOR A TUMOR LOCATED 4.7 CM FROM THE ANTENNA ARE PRESENTED FOR THE MORE REALISTIC HEMISPHERICAL AND SIMPLER CYLINDRICAL MODELS.

Signal processing step	Peak-to-peak ratio (dB)	
	Realistic	Cylindrical
Initial signal	-104.2	-105
Calibration	-51.3	-53.1
Skin subtraction	-11.34	-18.9
Integration	-17.5	-23.3
Compensation	-8.5	-5.66

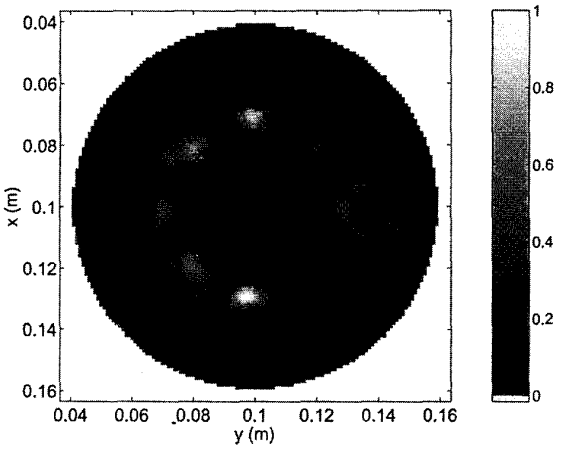

Fig. 2. 2D slice (xy plane) through the hemispherical model with a tumor at x=0.125 m, y=0.1 m. The image is reconstructed with 20 antennas.

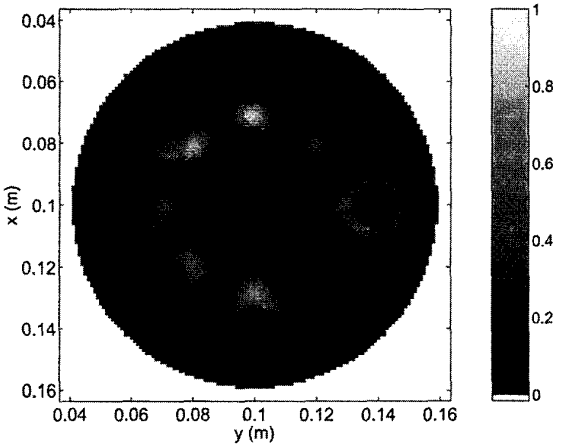

Fig. 3. 2D slice through hemispherical model without tumor.

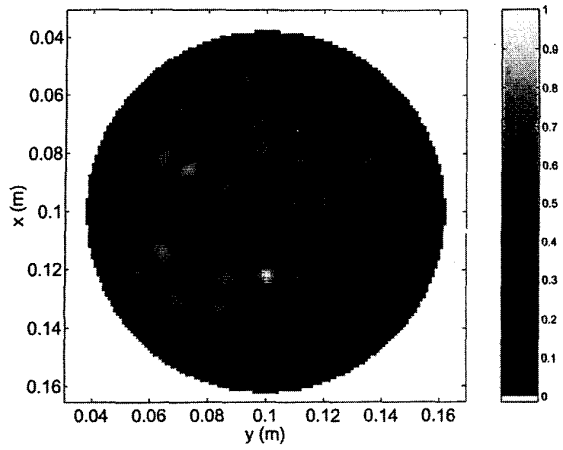

Fig. 4. Cut through xy plane of 3D reconstructed data at the maximum tumor response location.

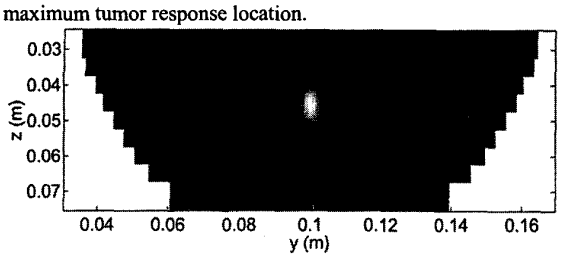

Fig. 5. Cut through yz plane of 3D reconstructed data at the maximum tumor response location.

IV. Discussion

Table 1 indicates that the peak-to-peak tumor responses for the hemispherical model are comparable to those obtained with simple models. The hemispherical model has larger diameter, and detection in this larger diameter model is challenging, as small responses are received from tumors that are further away from the antennas. For example, the initial peak-to-peak ratio for the antenna at 10.2 cm indicates that measuring the response of tumors at greater distances is difficult. It may be practical to form images of sections of the breast closest to a given set of antennas.

Figs. 2 and 3 demonstrate the increased clutter encountered with the hemispherical breast models. Tumor detection is possible, however false alarms are present. Comparison of these figures indicates that, with sufficient symmetry, subtraction or comparison of right and left breast images may improve tumor detection.

The results of the 3D scan indicate that including the local subtraction reduces clutter without eliminating the tumor response. The tumor response is shifted slightly from the physical location, as propagation velocity is estimated based only on the properties of fat tissue. The response is well localized in the xy plane, and less localized in yz plan due to the 4.5 cm span of synthetic array along the z axis. Figs. 4 and 5 show that, even with local subtraction, clutter in the image remains significant, suggesting that improved clutter reduction techniques are required.

Finally, the reconstructed images represent a section of the breast located away from the chest wall. A method to scan the antennas close to the chest region and to image the upper outer quadrant of the breast is required for a complete scan.

V. Conclusions

It appears feasible to detect and localize tumors in scans of more complex 3D breast models. Clutter is a more significant issue than with simpler models, suggesting the adaptation of more sophisticated clutter reduction techniques to this problem. Future work with the cylindrical CMI system includes developing methods to perform a 3D scan of the entire region of interest.

Acknowledgement

The authors would like to thank Dr. S.C. Hagness, Ms. Xu Li, and Dr. M.A. Stuchly for their support. This work was supported an NSERC postdoctoral fellowship.

References

[1] *Mammography and Beyond: Developing Technologies for the Early Detection of Breast Cancer*, Committee on Technologies for the Early Detection of Breast Cancer, Sharyl J. Nass, I. Craig Henderson, and Joyce C. Lashof, eds., National Cancer Policy Board, Institute of Medicine, and Commission on Life Studies, National Research Council, 2001.

[2] P.M. Meaney, M.W. Fanning, D. Li, S. P. Poplack, and K.D Paulsen, "A clinical prototype for active microwave imaging of the breast," *IEEE Trans. Microw. Theory Tech.*, vol. 48, 2000, pp. 1841-1853.

[3] E.C. Fear, X. Li, S.C. Hagness and M.A. Stuchly, "Confocal microwave imaging for breast cancer detection: localization of tumors in three dimensions", *IEEE Trans. Biomed. Eng.*, accepted, Jan. 2002.

[4] X. Li and S. C. Hagness, "A confocal microwave imaging algorithm for breast cancer detection," *IEEE Microw. Wireless Components Lett.*, vol. 11, 2001, pp. 130-132.

[5] E.C. Fear and M.A. Stuchly "Microwave detection of breast cancer," *IEEE Trans. Microw. Theory Tech.*, vol. 48, 2000, pp. 1854-1863.

[6] A. Taflove and S.C. Hagness, *Computational Electrodynamics: The Finite Difference Time Domain Method, 2nd ed.*, Artech House: Boston, 2000.